Molecular Scale Imaging of F-Actin Assemblies Immobilized on a Photopolymer Surface

Taiji Ikawa,[1,2,*] Fumihiko Hoshino,[1] Osamu Watanabe,[1] Youli Li,[2,†] Philip Pincus,[2] and Cyrus R. Safinya[2,‡]

[1]*Toyota Central R&D Laboratories, Inc., Nagakute, Aichi, 480-1192, Japan*

[2]*Materials Research Laboratory, Departments of Materials, Physics, Molecular and Cellular, and Developmental Biology, University of California, Santa Barbara, California 93106, USA*

(Received 23 August 2006; published 3 January 2007)

A photo-immobilization based process is presented for direct imaging of hierarchical assemblies of biopolymers using atomic force microscopy (AFM). The technique was used to investigate the phase behavior of F-actin aggregates as a function of concentration of the divalent cation Mg^{2+}. The data provided direct experimental evidence of a coil-on-coil (braided) structure of F-actin bundles formed at high Mg^{2+} concentrations. At intermediate Mg^{2+} concentrations, the data showed the first images of the two-dimensional nematic rafts discovered by recent x-ray studies and theoretical treatments.

DOI: 10.1103/PhysRevLett.98.018101 PACS numbers: 87.16.Ka, 68.37.Ps, 82.35.Gh

Cytoskeletal filamentous (F-) actin, a double-stranded helical filament made of the protein *G*-actin, can be considered as a semiflexible and highly charged polyelectrolyte, with diameter $D_A \sim 80$ Å, persistence length $\xi_A \sim 10$ μm, and anionic liner charge density $\lambda_A \sim -e/2.5$ Å [1–3]. In vitro F-actin in the presence of divalent cations assembles into gel-like networks and bundles that resemble their cellular counterparts formed with linker proteins. The F-actin/divalent cation aggregation has been used as a good model system, both experimentally and theoretically, for studying biological polyelectrolyte association [4–11]. Recent experiments using high resolution small-angle x-ray scattering (SAXS) showed that with high concentration of divalent cations, F-actin forms bundles consisting of filaments that are closely packed in a distorted hexagonal arrangement [4,5]. Within a small range in the low cation concentration regime, a unique layered structure consisting of stacks of nematic F-actin rafts was observed [4]. The detailed structural phase behavior of the F-actin supramolecular assembly challenges present theoretical models in many aspects [9–11]. Clearly, in addition to the average structures revealed by x-ray diffraction, to have a detailed view of the individual structural elements (filaments, bundles, and networks) at the molecular level would provide much insight into the interactions that drive the self-assembly process of biological polyelectrolytes.

Although atomic force microscopy (AFM) has become an established technique for imaging biological macromolecules including single F-actin filaments [12–14], imaging protein assemblies in native environments present special challenges due to the concentration-dependent nature of the phase behavior. Here, we present a method that can be effectively used to image a wide range of supramolecular assemblies in native environments with molecular resolution. The technique, which is based on a recently developed molecular imprinting and immobilization technique using a photo-sensitive polymer containing an azobenzene group (azo-polymer) [15], was used to prepare F-actin–Mg^{2+} samples at multiple concentration points on a single substrate for AFM imaging, yielding a real space structural phase diagram in one experiment. The technique is well suited for biomolecular imaging, especially for AFM, providing a nonreactive, nonionic, and flat surface (the surface roughness can be <0.3 nm) on which the complex biomolecular assemblies can be immobilized with little conformational change in the native aqueous environment.

The experimental procedure is briefly described below. F-actin was polymerized from lyophilized monomeric Globular (*G*-) actin (2 mg/ml) from rabbit skeletal muscle [4,5]. F-actin length was controlled by the addition of an appropriate amount of 1 mg/ml gelsolin [4]. The azo-polymer, poly{4′-[[[2-(methacryloyloxy) ethyl]ethyl] amino]-4-cyanoazobenzene-co-methyl methacrylate} (15 mol% azobenzene moiety, molecular weight 25 000) was obtained by free-radical polymerization [15]. The photo-immobilization process used to prepare the F-actin–Mg^{2+} samples is shown in Fig. 1(a). F-actin, and magnesium chloride solutions are spotted (each spot contains 1 μl of $MgCl_2$ and 1 μl of F-actin) and mixed on the surface of a spin-coated azo-polymer film on a glass substrate. Each sample (substrate) contains an array of spots (typically 6–8) with different concentrations of F-actin and Mg^{2+}. The azo-polymer film was sealed inside a humidity chamber to prevent evaporation and irradiated for 60 minutes with light (470 nm) from a 6×10 array of blue light emitting diodes (LED) with an optical power density of 10 mW/cm^2. During photo-irradiation, the photo-isomerization motion of the azobenzene group and the resultant photo-plasticization of the polymer matrix lead to a deformation of the polymer surface along the contour of surface biomolecules and thus immobilize them [15,16]. After washing the surface to remove excess sample, the substrate was probed by using a Digital Instruments Dimension 30000 scanning probe microscope in tapping-mode with a standard silicon cantilever (tip radius of curvature $\sim$20 nm).

The immobilization process dramatically reduces the thermal motion of F-actin filaments, leading to higher

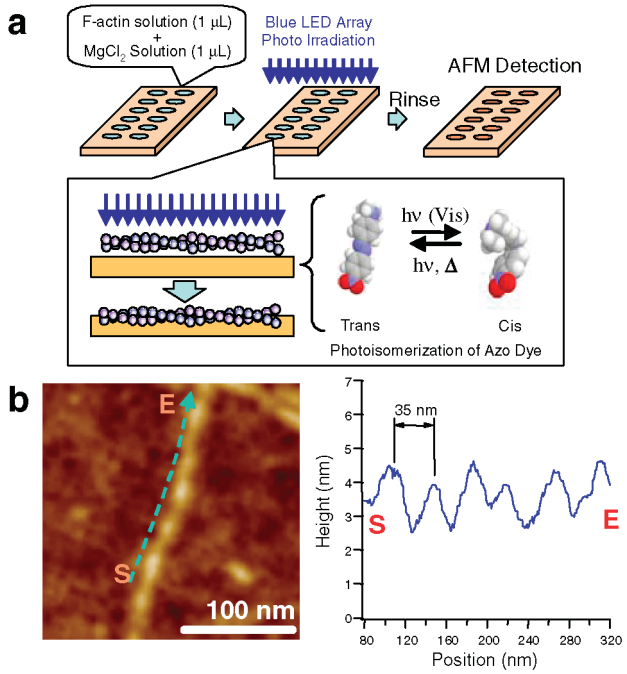

FIG. 1 (color). Photo-immobilization of F-actin–Mg^{2+} samples on an azo-polymer surface for AFM studies. (a) A schematic of the photo-immobilization process. Light irradiation induces the azo-polymer surface to deform along F-actin filaments due to the photo-isomerization motion of the azo-dye. (b) An AFM image of a single F-actin filament and a height trace along the single filament showing periodic variations corresponding to *G*-actin subunits.

imaging resolution allowing individual F-actin filaments to be resolved. Figure 1(b) shows an AFM image and an axial height trace of a single F-actin filament immobilized on the azo-polymer surface. The height trace shows periodic variation with a typical repeating distance of 35 nm matching the pitch of the F-actin. The observed pitch varies from 30 nm to 40 nm, which is consistent with previous electron microscopy observations that F-actin is a helix with a random variable twist [1,2,17]. The observed height (3 nm–4 nm from valley to peak) of the filament is about half of the actual F-actin diameter (6–8 nm), suggesting that the filament is about halfway embedded into the azo-polymer film after photo-immobilization. The typical observed width of a single filament measured perpendicular to the fiber is around 20 nm, about 3 times greater than the actual diameter of F-actin, which can be attributed to a tip-sample convolution effect [18]. Even though it is difficult to remove this tip-sample convolution effect, it is not difficult to differentiate between single filaments and bundles based on their apparent diameter.

The multiple-spot geometry allowed us to investigate F-actin assemblies as a function of increasing cation concentration on a single sample with relative ease. Figures 2(a)–2(c) demonstrate the progressive association of long actin filaments (up to ~10 μm in length, no gelsolin) with increasing Mg^{2+} concentration (0 m*M*, 10 m*M*, 80 m*M*, respectively) on the azo-polymer surface. The F-actin solution with 0 m*M* Mg^{2+} exhibits an uncondensed isotropic phase [Fig. 2(a)], with filaments maintaining large distances and intersecting angles (~90 degrees) between them to minimize electrostatic repulsion [11,19]. With 10 m*M* Mg^{2+} [Fig. 2(b)], the distances between filaments become smaller and the filaments form a network structure with smaller intersecting angles between filaments. The network consists of predominantly single filaments of F-actin. At 80 m*M* Mg^{2+} [Fig. 2(c)]; however, a different network structure composed of mostly thick filaments (F-actin bundles) is observed. The single filaments and bundles are entangled and oriented randomly in the network, suggesting little excluded volume interaction which drives liquid crystalline ordering in the more concentrated solution. Interestingly, the bundles observed in the networks appear to be fairly uniform in diameter and large bundles were rarely seen under this condition. This suggests that there might be a growth limit of the bundle size, which has been predicted theoretically [20]. Overall, the phase behavior observed in the AFM images is consistent with the previous results obtained using x-ray diffraction and optical microscopy [4]. However, the high resolution data allowed us to examine the structures at a single filament or bundle level, which led to observations

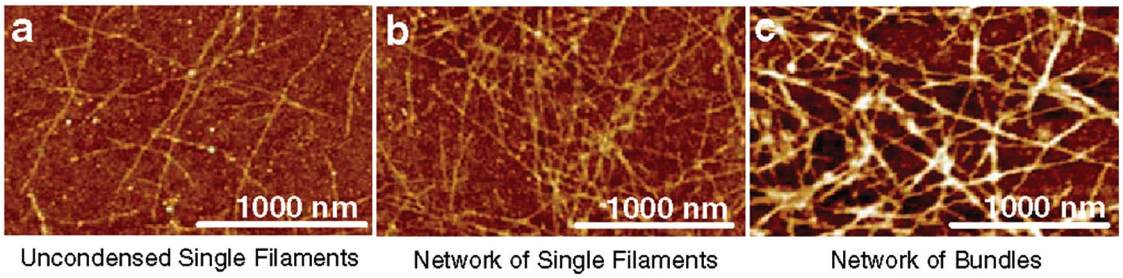

FIG. 2 (color). AFM images showing the progressive association of long (no gelsolin) actin filaments as a function of Mg^{2+} concentration. (a) Isotropic phase of F-actin filaments (0 m*M* Mg^{2+}). (b) Network of F-actin filaments (10 m*M* Mg^{2+}). (c) Network of F-actin bundles (80 m*M* Mg^{2+}). The phase map was obtained from one azo-polymer sample containing multiple spots of F-actin–Mg^{2+} mixed at different ratios.

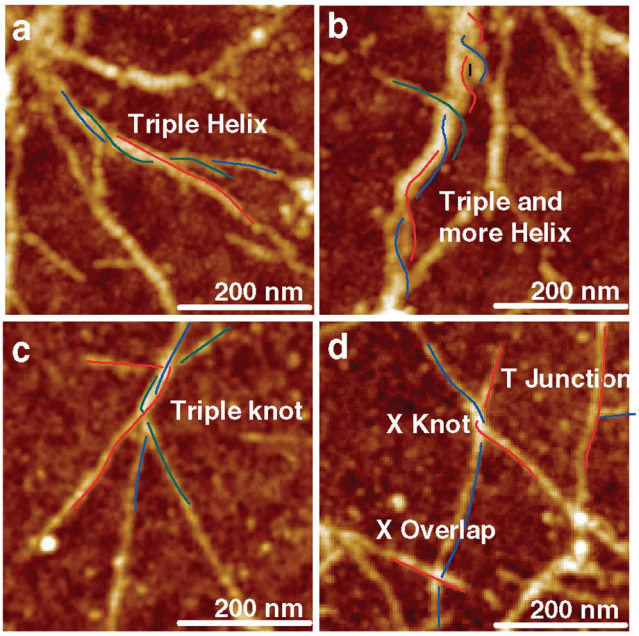

FIG. 3 (color). Braided structures of short F-actin (average length 680 nm) bundles and precursor junctions. (a, b) Braided bundles at high concentration of Mg^{2+} (80 mM). The bundle in image (a) consists of three filaments, and the bundle in (b) consists possibly of more than three filaments. (c, d) Junction-type precursor structures formed in the uncondensed phase of F-actin with 5 mM Mg^{2+}. All the images are 0–10 nm in height.

relevant to several important unanswered questions about F-actin assemblies.

There has been much discussion about the structure of bundles that are formed by charged biopolymers at high counterion concentrations. One of the intriguing possibilities is whether the F-actin filaments could form helical coil within a bundle [14]. Analogous structures have been theoretically predicted [21,22], but never experimentally verified. Using the current technique, we have found direct evidence of the coil-on-coil (braided) bundle structure at higher cation concentrations (>20 mM Mg^{2+}). In Figs. 3(a) and 3(b), we show two examples of the braided bundles formed with short F-actin (average length = 680 nm controlled with gelsolin) and 80 mM Mg^{2+}. Under this condition, we observed coexistence of both single filaments and bundles, which can be easily differentiated in the magnified images by their apparent diameter. Following the trace lines, it can be seen that the bundles unravel at their ends into three or more single filaments. The braided configuration of the bundle is especially obvious in Fig. 3(b). The braided structure is found to exist in a wide range of Mg^{2+} concentrations (5 mM to 160 mM), from the uncondensed phase to the bundled phase. In comparison, such spiral structures were not readily discernible in the bundles that are formed by longer filaments [Fig. 2(c)]. One could argue that the longer filaments are more prone to kinetic hindrance to forming braided structures due to increased difficulty in rotational movements.

AFM images of F-actin at lower Mg^{2+} concentrations offered some clues as to how the helical bundles may be formed. Figures 3(c) and 3(d) show several distinct F-actin junctions (points where single filaments are joined or crossed) observed at 5 mM Mg^{2+} concentration. In Fig. 3(c), three filaments form a knot structure of about 100 nm in length, and the knot unravels at both ends into three single filaments with fairly large angular separation. Also, entangled points formed by two filaments are observed in Fig. 3(d). In the same image, two other types of joints could be seen: an X overlap in which the two filaments simply cross each other and a T junction where the end of one filament is seemingly attached to another filament at a near 90 ° angle. All these junctions can be considered as precursor sites of the more extensive helical bundle structure shown in Figs. 3(a) and 3(b) at higher Mg^{2+} concentrations.

The braided bundle structure may have been present in previous images of F-actin bundles obtained using electron microscopy, AFM, and confocal optical microscopy, but was not recognized as such. For example, high resolution cryo-AFM images of F-actin filaments clearly showed the existence of braided bundles [14]. Synchrotron x-ray diffraction data showed that the close packing pattern of the bundle deviates from an exact hexagonal arrangement ($q_{10} = 0.089$ Å^{-1} and $q_{11} = 0.139$ Å^{-1}, respectively), which may be partially attributed to the braided arrangement of some F-actin filaments inside the bundle [4,5]. The observed axial repeat distance of the braided bundles is around 100 nm (Fig. 3(b) and 3(c)), comparable to the pitch of a single F-actin twisted structure. This strongly suggests that the F-actin filament follows the topology of the twist of F-actin filaments in order to achieve tighter packing.

It is important to note that the existence of braided F-actin bundles does not necessarily contradict the earlier conclusion of hexagonal packing of filaments inside the bundles. Because of the limited statistical sampling of AFM imaging and the large F-actin length distribution, it is likely that the actual samples contain both structures,

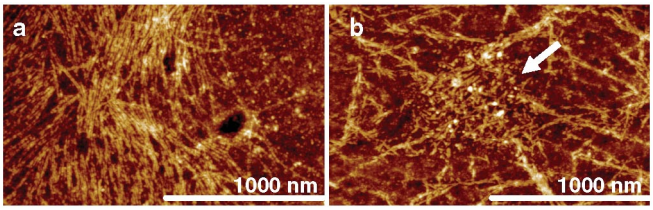

FIG. 4 (color). AFM images of intermediate phases of short F-actin (average length 170 nm) Mg^{2+}. (a) A phase consists of nematiclike rafts with 20 mM Mg^{2+}. In part, the rafts are stacked. (b) A phase consists of both perpendicular aggregates (arrow) and nematiclike rafts with 10 mM Mg^{2+}.

with hexagonal bundles being the prevalent structure giving rise to the x-ray diffraction peaks.

The structures formed in the intermediate range of concentration are of particular interest, as previous x-ray studies revealed in this regime a unique phase composed of lamellar stacks of crossed rafts (L_{XR} phase) [4]. Such a structure, formed with 20 mM of Mg^{2+}, is shown in Fig. 4(a). The filaments form a 2D nematiclike rafts with a lateral repeat distance of about 12 nm, slightly larger than the F-actin diameter. The rafts are stacked at a large angle from each other, as was deduced from x-ray data, which showed a series of strong (00L) harmonic peaks due to stacking. The raftlike structures can be observed in a wide range of Mg^{2+} concentration (5–40 mM) with short F-actin filaments and were much less dominant with longer filaments. This is consistent with the phase diagram compiled with x-ray data [4]. Similar structure has been observed in the system consisting of microtubules and divalent cations [23], suggesting a certain degree of universality of phase behavior of rodlike biological filaments with divalent cations. The 2D nematiclike rafts were found to coexist with aggregated perpendicular filaments at slightly lower Mg^{2+} concentrations (5–10 mM), as shown in Fig. 4(b), which is consistent with recent molecular dynamic simulation predictions that isolated stiff polyelectrolyte filaments in general evolve from aggregated perpendicular filaments to aggregated parallel rods [11]. The theoretical treatment also describes that the aggregated perpendicular filaments can form two-dimensional rafts [10].

A new protein immobilization technique was developed for molecular scale imaging by AFM of F-actin supramolecular structures formed in the presence of Mg^{2+}. The technique allowed combinatorial investigations of the phase behavior of the F-actin–Mg^{2+} system and revealed new structural details relevant to the understanding of cation-induced biopolymer aggregates. We found, in particular, a predominantly three-filament helical coil-on-coil structure in the F-actin bundles at higher divalent cation concentrations. The existence of the layered, raftlike F-actin structure at intermediate cation concentration, first revealed by x-ray diffraction, was confirmed unambiguously.

This work is supported by DOE No. DE-FG02-06ER46314, NSF Nos. DMR-05003347 and CTS-0404444, ONR No. N00014-05-1-0540, and MEXT KAKENHI (18550163). We thank L. S. Hirst, N. Bouxsein, K. Evert, and K. Kawamoto for useful discussions and help with sample preparation.

*Corresponding author: Toyota Central R&D Laboratories, Inc., Nagakute, Aichi, 480-1192, Japan. Electronic mail: e1056@mosk.tytlabs.co.jp

†Corresponding author: Materials Research Laboratory, University of CA, Santa Barbara, CA 93106. Electronic mail: youli@mrl.ucsb.edu

‡Corresponding author: Materials Department, University of CA, Santa Barbara, CA 93106. Electronic mail: safinya@mrl.ucsb.edu

[1] U. Aebi, R. Millonig, H. Salvo, and A. Engel, Ann. N.Y. Acad. Sci. **483**, 100 (1986).
[2] E. H. Egelman, Curr. Biol. **14**, R959 (2004).
[3] B. Alberts *et al.*, *Molecular Biology of the Cell* (Garland Science, New York, 2002), 4th ed..
[4] G. C. L. Wong, A. Lin, J. X. Tang, Y. Li, P. A. Janmey, and C. R. Safinya, Phys. Rev. Lett. **91**, 018103 (2003).
[5] T. E. Angelini, H. Liang, W. Wriggers, and G. C. L. Wong, Proc. Natl. Acad. Sci. U.S.A. **100**, 8634 (2003).
[6] K. Yamamoto, M. Yanagida, M. Kawamura, K. Maruyama, and H. Noda, J. Mol. Biol. **91**, 463 (1975).
[7] H. Strzelecka-Golaszewska, E. Prochniewicz, and W. Drabikowski, European Journal of Biochemistry **88**, 219 (1978).
[8] J. X. Tang and P. A. Janmey, J. Biol. Chem. **271**, 8556 (1996).
[9] B.-Y. Ha and A. J. Liu, Phys. Rev. Lett. **79**, 1289 (1997).
[10] I. Borukhov and R. F. Bruinsma, Phys. Rev. Lett. **87**, 158101 (2001).
[11] K.-C. Lee, I. Borukhov, W. M. Gelbart, A. J. Liu, and M. J. Stevens, Phys. Rev. Lett. **93**, 128101 (2004).
[12] H. G. Hansma, Annu. Rev. Phys. Chem. **52**, 71 (2001).
[13] T. Lehto, M. Miaczynska, M. Zerial, D. J. Müller, and F. Severin, FEBS Lett. **551**, 25 (2003).
[14] Z. Shao, D. Shi, and A. V. Somlyo, Biophys. J. **78**, 950 (2000).
[15] T. Ikawa, F. Hoshino, T. Matsuyama, H. Takahashi, and O. Watanabe, Langmuir **22**, 2747 (2006).
[16] A. Natansohn and P. Rochon, Chem. Rev. **102**, 4139 (2002).
[17] E. H. Egelman, N. Francis, and D. J. DeRosier, Nature (London) **298**, 131 (1982).
[18] P. Markiewicz and C. Goh, J. Vac. Sci. Technol. B **13**, 1115 (1995).
[19] S. L. Brenner and V. A. Parsegian, Biophys. J. **14**, 327 (1974).
[20] B.-Y. Ha and A. J. Liu, Europhys. Lett. **46**, 624 (1999).
[21] Y. Snir and R. D. Kamien, Science **307**, 1067 (2005).
[22] R. D. Kamien and D. R. Nelson, Phys. Rev. Lett. **74**, 2499 (1995).
[23] D. J. Needleman, M. A. Ojeda-Lopez, U. Raviv, H. P. Miller, L. Wilson, and C. R. Safinya, Proc. Natl. Acad. Sci. U.S.A. **101**, 16 099 (2004).